Spatio-Temporal Image Correlation Spectroscopy Measurements of Flow Demonstrated in Microfluidic Channels

Molly Rossow[1], **William W. Mantulin**[2], and **Enrico Gratton**[3]

1*University of California Irvine, Biomedical Engineering Department, 3120 Natural Sciences 2, Irvine, CA 92697-2715, Phone: 949-824-3264, Fax: 949-824-1727, Email: rossowm@uci.edu*

2*University of California Irvine, Beckman Laser Institute, 1002 Health Sciences Rd, Irvine, CA 92612, Phone: 949-824-8859, Fax: 949-824-1727, Email: mantulin@uci.edu*

3*University of California Irvine, Biomedical Engineering Department, 3120 Natural Sciences 2, Irvine, CA 92697-2715, Phone: 949-824-2674, Fax: 949-824-1727, Email: egratton@uci.edu*

Abstract

Accurate blood flow measurements during surgery can improve the operations chance of success. We developed Near-infrared Spatio-Temporal Image Spectroscopy (NIR-STICS), which has the potential to make blood flow measurements that are difficult to accomplish with existing methods. Specifically, we propose the technique and we show feasibility on phantom measurements. NIR-STICS has the potential of measuring the fluid velocity in small blood vessels (less than 1mm in diameter) and of creating a map of blood flow rates over an area of approximately $1cm^2$. NIR-STICS employs near-infrared spectroscopy to probe inside blood vessel walls and spatio-temporal image correlation spectroscopy to directly—without the use of a model—extract fluid velocity from the fluctuations within an image. Here we present computer simulations and experiments on a phantom system that demonstrate the effectiveness of NIR-STICS.

Keywords

blood flow; image correlation; microfluidic channels

1 Introduction

It is important for surgeons to measure blood flow in exposed blood vessels during surgery. Impeded blood flow, even in small blood vessels, can cause serious damage to tissue and organs. The success of an operation and even the life of the patient may be at risk. Blood clots are a major cause of impeded blood flow during surgery. These clots can form when a blood vessel is intentionally, and temporarily, occluded in order to minimize bleeding. Once the surgeon releases the obstructed blood vessel it is imperative to determine if blood flow has been adequately reestablished. If it has not, there are steps the surgeon can take to correct the problem, such as removing a clot. In this situation, the surgeon's ability to protect the patient's well being relies on fast and accurate flow measurement.

A variety of technologies exist for measuring and quantifying blood flow. Each technique has its area of application and its limitations.[1] Doppler based techniques are one important category. There are two main subcategories of Doppler techniques: laser Doppler and ultrasonic Doppler. In both cases, radiation is directed towards the moving blood and the wavelength of the reflected radiation is measured.[2,3] The Doppler Effect causes the reflected radiation to have a different wavelength from the incident radiation. This difference in wavelength, the Doppler shift, is used to detect the fluid velocity. Doppler based techniques

are useful in that they give results quickly, are non-invasive and can even make measurements through the skin.[4,5,6]

However, there are also limitations to Doppler techniques. One drawback is that these techniques are only appropriate for larger blood vessels with faster flow rates and therefore large, easy to detect, Doppler shifts. Another limitation is that Doppler measurements are most suited to measurements at a single location, although scanning can extend their use to larger areas.[7]

Ultra-sonic transit time is another method that directly measures flow rate, not fluid velocity. [8] In this technique a pair, or several pairs, of ultrasonic transducers are placed on opposite sides of the blood vessel with one transducer in each pair downstream from the other. An ultrasonic wave is transmitted between the transducers. The flow rate is related to the time it takes the sound waves to traverse the vessel. This technique is valuable because it is currently the only way to directly measure the flow rate, as opposed to fluid velocity. Flow rate is directly related to the level of oxygenation the tissue receives. The other techniques calculate flow rate based on the cross section of the blood vessel. However, like Doppler based techniques, this technique is most suited to larger vessels. Additionally, among the techniques described here, it is one of the most invasive since the underside of the blood vessels needs to be exposed.

Another common technique involves the use of contrast agents. Contrast agents fall into two primary groups: fluorescent dyes such as fluorescein and indocyanine green and radioactive substances such as ^{133}Xenon. These substances are injected into the blood stream and the fluorescence or radiation they emit is observed to track blood flow. Fluorescent contrast agents are used in conjunction with an illumination source and provide a visual, qualitative fluid velocity over an area. Radioactive contrast agents are used to measure an average perfusion throughout an organ. Contrast agents do not give detailed, quantitative results and can only be used a limited number of times before the vessels are saturated with dye or patient safety is compromised.

Laser speckle is a technique that is still under development.[9,10] In this type of measurement a laser beam is directed at the blood vessel. The scattered radiation will have constructive and destructive interference. As the flow of blood moves the individual blood cells, the interference pattern in the reflected light fluctuates. The fluid velocity can be determined by interpreting these fluctuations using a theoretical model of flow and reflected light. Laser speckle is basically a point measurement technique, but, like Doppler techniques, it can be applied sequentially to multiple points. Another limitation of laser speckle is that it cannot provide information on the direction of flow since each speckle measurement is an average of the fluctuations within the area illuminated by the laser beam. The optics required for laser speckle have some similarities to the technique presented here, but they are distinct methods with very different data analysis approaches.

We propose a blood flow measurement technique, near-infrared spatio-temporal image correlation spectroscopy (NIR-STICS) that draws on both near-infrared spectroscopy and spatio-temporal image correlation (STICS) developed by Hebert *et al.*[11] This method is based on subtle intensity fluctuations, which are due to the underlying motion of blood cells. NIR-STIC has the potential to overcome some of the limitations of existing techniques, including laser speckle. NIR-STICS is non-contact and does not require the use of contrast agents, making it potentially safer for patients. Also, this method is capable of making measurements over an area, giving a map of the fluid velocities at different locations. Perhaps more significantly, the area examined can be close to a square centimeter in size, something that cannot be accomplished with laser speckle. Additionally, NIR-STICS provides the direction of flow and can distinguish between laminar and turbulent flow. NIR-STICS is fast and quantitative. In the

current implementation results can be obtained in under a minute and future improvements could yield results in a few seconds. Although in a developmental stage, this method can be extended to a surgical environment. The basic components—light source, camera, objective lens, and computer—are all already used in commercially available surgical microscopes. Overall, this technique improves upon many features of existing technology for measuring blood flow.

In this manuscript we describe the instrumentation required for NIR-STICS and the development of the data analysis approach. We focus on extracting flow information from STICS analysis. We present computer simulations of preliminary data using a microchannel tissue phantom to validate the feasibility of this approach.

2 Materials and Methods

2.1 Blood Flow Phantom

All flow measurements presented here were performed using a phantom system in which transparent channels represented blood vessels and whole milk represented blood. The smallest of these channels where on the order of 100μm wide and 100μm deep and were constructed from Polydimethylsiloxane (PDMS) using soft lithography procedures as described by Raguin *et al.*[12] This type of phantom is an established model of blood vessel networks and has been used in MRI experiments and tissue engineering research.[12,13] In our experiments two different microfabricated phantoms were used: one with a single channel to determine the instrument's accuracy in measuring fluid velocity and another with 2 independent channels to test the instrument's ability to measure different flows over an area. An additional phantom consisting of a tube approximately 4mm in diameter was used for experiments concerning laminar and turbulent flow. Turbulent flow was induced by partially clamping the tube so the fluid was forced from a large diameter tube into a smaller one, forming eddies.

In all phantoms whole milk was used as a model for blood. The fat globules in homogenized milk are similar in size to erythrocytes: both are approximately 10 μm in diameter. Fat globules are mostly spherical whereas erythrocytes are not. However, particle size and shape will not directly impact our fluid velocity measurements as will be discussed later. The use of milk in phantom studies has been established in the field of photon migration where experiments are performed using milk as a substitute for biological tissue.[14] In the experiments presented here the rate of flow was controlled by a syringe pump (KDS100, KD Scientific, Holliston, MA). This pump is capable of producing flow rates ranging from 0.04mL/hr to 80mL/hr in increments of 0.01mL/hr which includes the physiological range.

2.2 Optical Equipment

The blood flow phantom was illuminated using a 120W Mercury Vapor Short Arc (X-Cite 120Q Series, Ontario Canada), an incoherent, white light source. In a medical application of this technique a near-infrared light source would be used since biological tissue is more transparent in that spectral region. The use of an incoherent light source sets this technique apart from laser speckle technique, which, as the names implies, uses a coherent light source. In theory, a coherent light source could be used for our application as well. However, in practice we have observed that the speckle pattern created from reflected laser light overwhelms all other fluctuations making laser illumination impractical.

A CCD camera (PL-A661, Pixelink, Ottawa, ON, Canada) was used to detect the reflected light from the phantom's surface. The image per se does not show the blood cells. However, the intensity fluctuations carry information about the underlying movement of the particles. We extract the velocity from an analysis of the underlying fluctuations. Images were acquired

at a frame rate between 50 and 120 frames per second. All data and simulations presented here are the result of analyzing 128 frames. In order to optimize light collection, the camera was positioned at 90 degrees from the light source. Both the camera and the light source were positioned at 45 degrees from the surface. This arrangement is shown in Figure 1. In a typical measurement a 1X objective (Mitutoyo, Kawasaki, Japan) was placed in front of the camera to image an area of 8mm by 6mm on to a region 800 pixels by 600 pixels, at higher frame rates the pixel numbers were decreased.

Another element of the optical equipment was a pair of polarizers, one in the illumination path and one in the detection path. Cross-polarizers were used to increase contrast. This is necessary because a higher percentage of the detected light is reflected from the surface of the phantom or blood vessel than from the particles flowing inside. Using polarized light makes it possible to enhance the signal from the underlying moving particles

2.3 Computer Simulations

Simulations were performed to evaluate the STICS analysis method described below for flow measurement. In these simulations particles were represented as uniform disks moving in two dimensions. Fluid velocity was assumed to be constant throughout the observation volume (i.e. boundary effects were ignored) and was modeled as a displacement in the x direction at each time step of the simulation. Diffusion was included in this model as pseudo-random displacements in the x and y directions. This pseudo-random displacement was generated from a normal distribution with a mean of zero and a standard deviation of $\sigma = \sqrt{2 D \tau}$, where D was the diffusion coefficient in pixels^2/frame and τ is the frame time. Simulations were performed both in an ideal conditions and with both shot noise and constant background. All simulations were performed using Matlab version 7.3.0.267 (R2006b) (Matlab, Mathworks, Natick, MA).

The values of the parameters used in these simulations expressed in terms of pixels are as follows: each simulated image was 256 pixels by 256 pixels and the sub-region analyzed was 64 pixels by 64 pixels. The radius of the simulated particles was 2 pixels but 1 pixel gives similar results. The diffusion coefficient was 0.1 pixels^2/frame. The direction of flow was in the positive x direction. The velocity of the particles was varied from 0 to 15 pixels/frame. These values can be considered to model data acquired in the manner presented in this manuscript. The analyzed area is the same size for both simulated and actual data.

3 STICS Analysis

3.1 Basic Theory

The challenge in measuring flow by intensity fluctuations is that these fluctuations are combined with other, large, irrelevant signals, namely stationary objects, as illustrated in Figure 2, and camera noise. This is why the flow rate is not immediately obvious when looking at a series of images and why statistical analysis methods must be employed. Specifically, we use spatio-temporal image correlation analysis (STICS.) The technique presented here is a modified version of the STICS analysis developed by Hebert *et al.*[11] In this analysis, the signal from stationary objects is removed first, through subtraction of the average image. The camera noise is removed through correlation techniques. Camera noise, in our system, does not correlate spatially or temporally and therefore is not present in the correlation results.

Subtracting the temporal average of all images from each image eliminates the signal from any stationary objects in the field; otherwise the correlation from stationary objects overwhelms the correlation signal from the moving object we are interested in. Subtraction of the average image has the consequence of changing the average intensity of each frame. This will in turn

change the amplitude of the correlation. This method of removing stationary components is different from low-pass filtering method used by Hebert

he STICS calculation is defined in equation 1.[11]

$$G_{\text{STICS}}(\xi,\psi,\Delta T)=\left\langle \frac{\langle \delta i_a(x,y,t)\, \delta i_b(x+\xi,y+\psi,t+\Delta T)\rangle_{x,y}}{\langle i_a(x,y,t)\rangle_{x,y}\langle i_b(x,y,t+\tau)\rangle_{x,y}} \right\rangle_t$$

(equation 1)

Where i_a and i_b are the intensities at each pixel of image a and image b respectively. x and y are the horizontal and vertical spatial coordinates. ξ and ψ are the x and y spatial correlation shifts. t is the frame number and ΔT is the shift between frames. $\delta(\dots) = i - \langle i \rangle$ and $\langle\ \rangle_{x,\,y}$ is the average intensity of the image. We calculate STICS using the Fast Fourier Transform to improve data processing speed.

STICS is based on spatial correlations. The spatial cross-correlation function provides a method of mathematically evaluating the similarity between images. It is highest in value at spatial shifts (ξ and ψ) for which the second image ($i_a(x,y)$) is similar in intensity to the first ($i_b(x, y)$). That is to say it has a high value when the intensity of image a at location (x,y) is similar to the intensity of image b at location ($x + \xi, y + \psi$). A useful representation of a spatial correlation function, which is used here, is a two dimensional plot in which the axes are ξ and ψ and the magnitude of the function is represented with a color scale.

The spatial cross-correlation function is particularly useful for extracting information about flow because there is a high degree of similarity between sequential images of flowing particles and spatial cross-correlation analysis responds to this. Each particle in one image moves to a new location in the next image and so on. The particle appears at a greater spatial shift in each successive image. This means that each image is essentially a shifted version of the earlier images. The displacement caused by flow will be approximately the same for each particle since flow moves all particles in the same direction at the same rate. Therefore, for G calculated between two successive images of flowing particles, there will be a peak in the spatial correlation function at a spatial shift equal to the displacement caused by flow.

In STICS analysis the cross correlation is calculated between all pairs of images with a fixed time shift (ΔT) between them. For example, at $\Delta T = 2$ frame 1 is correlated with 3, frame 2 with frame 4, frame 3 with frame 5, etc.). These cross correlations are then averaged. STICS can be calculated at more than one time shift ($\Delta T = 0$, $\Delta T = 1$, $\Delta T = 2$ etc.). Larger shifts should give the most accurate measurement of flow since they include position at longer time delays however, this is limited by diffusion and particles that move out of frame. We calculate STICS at multiple time shifts to obtain the maximum amount of temporal information and to improve the accuracy of the flow rate obtained through fitting the data as described below.

3.2 Extracting Velocity from STICS

The peak value of the STICS correlation plot is shifted from the center in the direction of flow by an amount that relates to the speed at which the particles are traveling. Average velocity can be extracted as described in equation 2

$$v=\frac{\text{ObservedPixelShift} \times \text{PixelWidth}}{\left(\frac{1}{\text{frameRate}}\right)\Delta T}$$

(equation 2)

More precise numerical information is extracted from STICS analysis by fitting the experimental STICS plot to a 2-dimensional Gaussian (equation 3.)

$$z = Ae^{-\left[\frac{(x-\mu_x)^2}{2\sigma_x^2} + \frac{(y-\mu_y)^2}{2\sigma_y^2}\right]}$$

(equation 3)

Where A is the amplitude. σ_x and σ_y are the standard deviation of the Gaussian in the x and y direction respectively and are related to the rate of diffusion. The variables μ_x and μ_y give the displacement of the peak in the x and y direction respectively at each ΔT. The observed pixel shift from equation 2 can be obtained from equation 3 through equation 4.

$$ObservedPixelShift = \sqrt{\mu_x^2 + \mu_y^2}$$

(equation 4)

The direction of flow can also be obtained from equation 3 through equation 5.

$$\theta = \tan^{-1}\frac{\mu_y}{\mu_x}$$

(equation 5)

where θ is the angle between the x axis and the direction of flow.

3.3 Mapping Flow

In the data presented here, STICS analysis and global data fitting was done in regions 32 pixels by 32 pixels that overlap by 16 pixels. Using a small area improves data processing speed. Additionally, it makes it possible to map flow by improving resolution. In the experimental data presented here each 32 pixel by 32 pixel analysis region corresponds to an area 0.32mm by 0.32mm meaning that the resolution of such a map is less than 1mm. The results of flow mapping are displayed using arrows to represent the velocity. One arrow is placed in the center of each region of analysis. The length of the arrow corresponds to the magnitude of the velocity as calculated in equations 2 and 4. The direction of the arrow corresponds to the direction of flow as determined using equation 5. Arrows are plotted for each region of analysis in which the amplitude of the STICS peak is above a threshold value.

3.4 Distinguishing Laminar and Turbulent Flow

Laminar and turbulent flow have distinct STICS plots when the region of analysis is large enough relative to the scale of the flow pattern. Laminar flow is characterized by velocities that vary spatially in magnitude but not in direction. This results in an STICS peak that is elongated in the direction of flow. Turbulent flow has a velocity pattern that varies both spatially and temporally in magnitude and direction. Turbulent flow often contains circulating regions or eddies. This type of flow causes the STICS peak to become wider as ΔT increases until it stabilizes at a maximum width. The peak will also move in the direction of the overall flow.

4 Results

4.1 Computer Simulations

The results presented here make clear that fluid velocity can be measured using STICS analysis. Representative results of the computer simulations can be seen in Figure 3. STICS analysis of

simulated data with a constant flow rate is presented at two different STICS shifts. The STICS plot on the left where the STICS shift is zero (T=0) does not provide any information about flow, since it is the average of the spatial autocorrelation of each frame (the cross-correlation of a frame with itself) and the location of the STICS peak does not change regardless of the velocity. The size of the STICS peak at T=0 is related to the size of the particles at small particle velocities. **Error! Bookmark not defined.Error! Bookmark not defined.**

The velocity can be extracted from the location of the peak at different ΔT using the simulation parameters and equations 2 and 3. A plot of this extracted velocity is shown in Figure 4. The method is accurate and only requires calibration to determine the size of the image. This can be accomplished by placing a ruler in the field of view.

4.2 Blood Flow Phantoms

In Figure 5 we show the peak of the STICS plot at $\Delta T = 5$ for two flow rates. At a flow rate of 0, the STICS peak is located at the origin and at a non-zero flow rate the location of the STICS peak moves farther from the center of the plot. Fluid velocity can be extracted from STICS analysis using the method described above. Figure 6 shows the extracted fluid velocity plotted versus the applied flow rate. The correlation coefficient between the two is R = 0.94.

4.3 Flow Mapping

The most important feature demonstrated by our experiments is that STICS can be used to map flow in multiple channels over an area. In Figure 7 STICS analysis was used to map flow in two different channels simultaneously with different flow rates as described in section 3.3. In the top channel, the flow rate is faster and this is reflected in the longer arrows.

4.4 Distinguishing Laminar and Turbulent Flow

An additional and potentially important implication of the STICS methods is that NIR-STICS could distinguish between turbulent and laminar flow as discussed in the Methods section. The most straightforward way this can be accomplished is through the mapping procedure described above. Complex flow patterns on a certain scale within a channel will be reflected in the range of velocities found over the area mapped. This type of flow mapping is accessible by other techniques including Doppler.[7] There is however, a more subtle and unique way STICS can distinguish between laminar and turbulent flow: the shape of the STICS peak is determined by the flow pattern *within* the region of analysis. Figure 8 contains an example of laminar and turbulent flow analyzed with STICS. The turbulent flow was obtained by partially obstructing the flow channel. The laminar flow plot is elongated in the direction of flow and it is asymmetrical. This reflects a particles moving at varying speeds but overall in the same direction within the region of analysis. The STICS plot for the turbulent flow is round and more symmetrical. This is due to particles moving in many directions locally (an eddy) but in one direction overall.

5 Discussion

5.1 Instrumentation Considerations

In the STICS technique measurements must be made with a frame rate and maximum ΔT that are appropriate for the velocity being measured. If the frame rate is too slow the particles will move out of the image before a second image is acquired and it will be impossible to recover the velocity. The need for a fast frame rate has to be weighed against taking measurements over a large area since using larger frame sizes will slow the frame rate. The exposure time also needs to be large enough to obtain a sufficient signal to noise ratio for the level of illumination. Increasing the exposure time will also slow the frame rate. The frame rate and

maximum ΔT must also be appropriate for the velocity being measured. At frame rates that are too slow and ΔT values that are too large for the velocity, the STICS peak will "wrap around" to the opposite side of the STICS plot and flow will appear to be in the opposite direction. For example, at a velocity corresponding to 10 pixels/frame in the positive x direction and a region of analysis of 32 pixels by 32 pixels the STICS calculation at $\Delta T = 1$ will be accurate with the peak located at $\xi = 10$. However when $\Delta T = 2$ the STICS peak will be located at $\xi = -13$. This problem can be identified by calculating STICS for several values of ΔT and observing if the apparent direction of flow varies.

It is important to realize that the key feature of the STICS plot is the peak. The background may also have features as can be seen in Figures 3, 5 and 8 and it is rarely equal to zero at every point but the amplitude of these features is several times less than the amplitude of the peak due to the moving particles. In Figure 5 for example, the amplitude of the peak is 9×10^{-5} while the highest point outside the peak is 3×10^{-5}. There is no pattern observed between data sets for these features and increasing the number of frames acquired further decreases the amplitude of the surrounding peaks.

STICS flow maps can be created with varying resolutions depending on the size of the region of analysis. Smaller regions of analysis give greater resolution and are faster to calculate but are also more sensitive to noise. Large regions of analysis average the flow rate over a larger area and are appropriate when the average flow through a region is needed.

The experiments present here were all performed on phantom systems that were designed to closely mimic physiological systems. The channels were the same size as the blood vessels of interest, flow rates were in the correct range and the scattering particles were similar in size to blood cells. However, there were limitations to this phantom system. One important limitation was that the material used to create the phantoms was transparent while actual tissue scatters lights. Actual tissue would add stationary objects to the measurement which the background subtraction step would remove. Phantoms were used to control the experimental parameters more precisely and to accurately test the performance of the technique.

5.2 Medical Applications of NIR-STICS

NIR-STICS is a robust statistical technique and could be adapted to map blood flow during surgery. The technique relies on optical signals. It is effective even when individual blood cells cannot be resolved by the microscope. The STICS analysis extracts the rate of flow from optical fluctuations caused by individual particles.

The range of velocities accessible to NIR-STICS is limited only by the frame rate of the camera and the size of the region being analyzed, which is in turn dependent on the magnification and the desired resolution of the flow map. With the parameters described here fluid velocities ranging from less than 1mm per second to 25mm per second can be measured. Blood flow in the human body typically ranges from millimeters per second in the capillaries up to a meter per second in large arteries.[15,16] Faster frame rates and larger frame sizes would allow measurement of faster velocities. Slower velocities could be measured by acquiring data over a longer time frame. NIR-STICS in its present implementation does not encompass the entire range of blood flow rates in the human body but does provide a way to measure slower velocities that are difficult to measure with Doppler techniques. Moreover, with the parameters used here, NIR-STICS measurements can be performed in near-real time.

In addition to accessing a range of fluid velocities, NIR-STICS can be adapted for blood vessels of different sizes. The resolution of the image analyzed through STICS is dependent only on the magnification used to create the image. Blood vessels as small as capillaries will be accessible to NIR-STICS. Flow through any blood vessel less than approximately half a

centimeter in diameter can be measure with this technique. Larger blood vessels will have higher fluid velocities and thicker vessel walls and are less suited to NIR-STICS measurements. Again, NIR-STICS makes previously difficult measurements possible through its effectiveness on smaller blood vessels.

Furthermore, NIR-STICS is suited to measuring blood flow because it is insensitive to small temporal variations in flow. This means that pulsatile variability will not diminish the accuracy of NIR-STICS measurements. Even in the case of blood cells moving through capillaries slowly, one at a time, NIR-STICS can still provide an accurate measurement of the average velocity.

NIR-STICS could be used as the basis of a device to measure blood flow in exposed blood vessels during surgery. Such an instrument would be an improvement over existing technology in that it is non-contact, does not require the use of contrast agents, and can create a map of flow over a relatively large area. Additionally, the optics are such that they can be easily incorporated into existing surgical microscopes.

In addition to measuring fluid velocity, NIR-STICS as applied in the reflection mode should be able to determine other information such as the concentration of moving particles in the observation volume. This could also have medical applications as the number of blood cells is directly related to the rate at which oxygen reaches tissue.

5.3 Distinguishing Laminar and Turbulent Flow

NIR-STICS also has the potential to address medical issues related to turbulent blood flow. Turbulence can be caused by vascular anomalies including aneurysms, plaques, and diseased heart valves. Identifying turbulent flow and understanding its underlying causes is important to treat these conditions. The ability to distinguish between laminar and turbulent flow is an inherent property of NIR-STICS. This makes NIR-STICS a potentially valuable tool for examining blood flow in large blood vessels as well as the smalls blood vessels that are the focus of the experiments presented here.

5.4 Comparison to Speckle

It is important to acknowledge the differences and similarities between NIR-STICS and laser speckle. While it remains to be seen what the true strengths and weaknesses of laser speckle are, it is clear that the NIR-STICS will have advantages in that it can determine the direction of flow and it can be used to map flow over an area. A single point speckle measurements takes several seconds. This can make scanning, and therefore mapping, impractical. An additional complication with speckle is that it requires a mathematical model to extract the flow rate from the rate of fluctuation. In STICS analysis, the average displacement between frames can be determined directly from the location of the STICS peak whereas in speckle techniques assumptions must be made to relate the time scale of speckle fluctuations to the rate of flow.

6 Conclusions

NIR-STICS is an imaging technique can create a map of fluid velocities over an area. The strength of this method lies in its ability to extract the flow rate from many, noisy optical signals. NIR-STICS is fundamentally different from other optical correlation techniques like speckle because it does not require the use of a model; NIR-STICS is purely a statistical method. The instrumentation required for NIR-STICS methods is straightforward and compatible with existing technology. STICS analysis can be applied to images acquired in existing systems, including surgical microscopes. We are refining NIR-STICS and working towards testing it on an animal model.

Acknowledgments

References

1. Woodcock JP. Physical Properties of Blood and their Influence on Blood Flow Measurement. Reports on Progress in Physics 1975;39:65–127.

2. Holloway, GA. Laser Doppler Measurement of Cutaneuos Blood Flow. In: Rolfe, P., editor. Non-Invasive Phyiological Measurements. Academic Press; London: 1983. p. 383

3. Roberts, VC.; Sainz, AJ. Ultrasonic Doppler Velocimetry. In: Rolfe, P., editor. Non-invasive Physiological Measurements. Academic Press; London: 1979. p. 349

4. Tritton, DJ. Physical Fluid Dynamics. Clarendon Press; Oxford: 1988.

5. Tabrizchi R, Pugsley MK. Methods of blood Flow measurement in the arterial circulatory system. Journal of Pharmacological and Toxicological Methods 2000;44:375–384. [PubMed: 11325580]

6. Briers DJ. Laser Doppler, speckle and related techniques for blood perfusion mapping and imaging. Physiol Meas 2001;22:R35–R66. [PubMed: 11761081]

7. Uranishi R, Nakase H, Sakaki T, Kempski OS. Evaluation of Absolute Cerebral Blood Flow by Laser-Doppler Scanning -- Comparison with Hydrogen Clearance. Journal of Vascular Research 1999;36 (2):100–105. [PubMed: 10213904]

8. Amin-Hanjani S, Meglio G, Gatto R, Bauer A, Charbel F. The Utility of Intraoperative Blood Flow Measurement During Aneurysm Surgery Using an Ultrasonic Perivascular Flow Probe. Operative Neruosurgery 2006;2:58.

9. Abbiss JB, Chubb TW, Pike ER. Laser Doppler anemometry. Optics & Laser Technology 1974;6(6): 249–261.

10. Briers JD, Fercher AF. Retinal blood-flow visualization by means of laser speckle photography. Invest Ophthalmol Vis Sci 1982;22(2):255–259. [PubMed: 7056639]

11. Hebert B, Costantino S, Wiseman PW. Spatiotemporal Image Correlation Spectroscopy (STICS) Theory, Verification, and Application to Protein Velocity Mapping in Living CHO Cells. Biophys J 2005;88(5):3601–3614. [PubMed: 15722439]

12. Raguin, LG.; Honecker, SL.; Georgiadis, JG. MRI velocimetry in microchannel networks. Microtechnology in Medicine and Biology; 3rd IEEE/EMBS Special Topic Conference; 2005. p. 319-322.2005

13. Borenstein JT, Terai H, King K, Weingberg EJ, Kaazemput-Mofrad MR, Vacanti JP. Microfabrication Technology for Vascularized Tissue Engineering. Biomedical Microdevices 2002;43:167–175.

14. Tanner K, Beitel E, D'Amico E, Mantulin WW, Gratton E. Effects of vasodilation on intrinsic optical signals in the mammalian brain: a phantom study. Journal of Biomedical Optics 2007;11(6):064020. [PubMed: 17212543]

15. Noon JP, Walker BR, Webb DJ, Shore AC, Holton DW, Edwards HV, Watt GCM. Impaired Microvascular Dilatation and Capillary Rarefaction in Young Adults with a Predisposition to High Blood Pressure. The American Society for Clinical Investigation 1997;99(8):1873–1879.

16. Sarkar S, Ghosh S, Ghosh SK, Collier A. Role of transcranial Doppler ultrasonography in Stroke. Postgrad Medical Journal 2007;83:683–689.
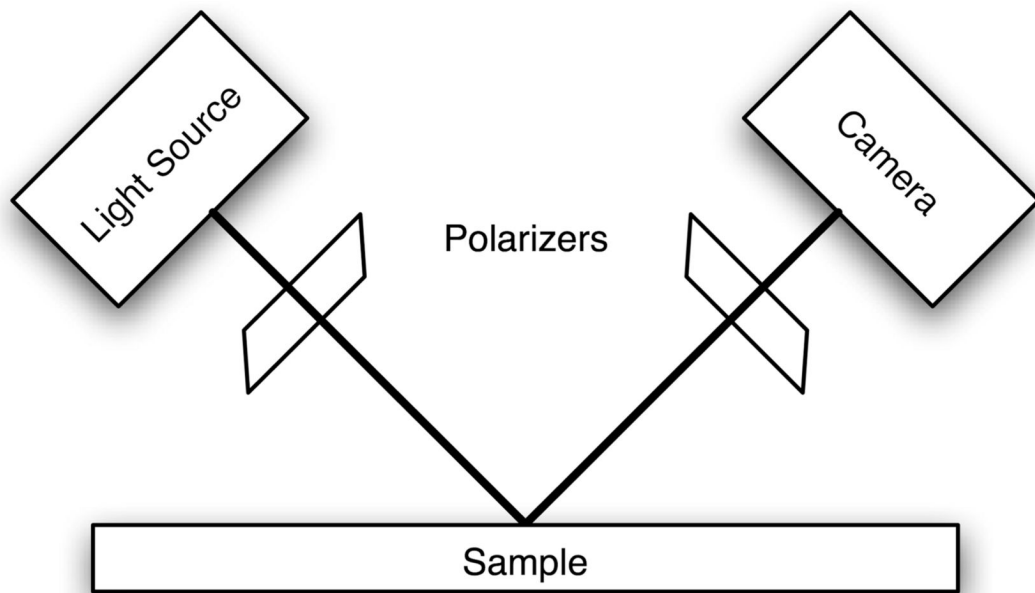
Figure 1.
Optical Equipment. The sample or blood vessel is illuminated with an incoherent, polarized, light source at a 45 degree angle to the surface. The reflected light is passed through a polarizer of the opposite orientation and collected by a 1X objective lens attached to a camera.
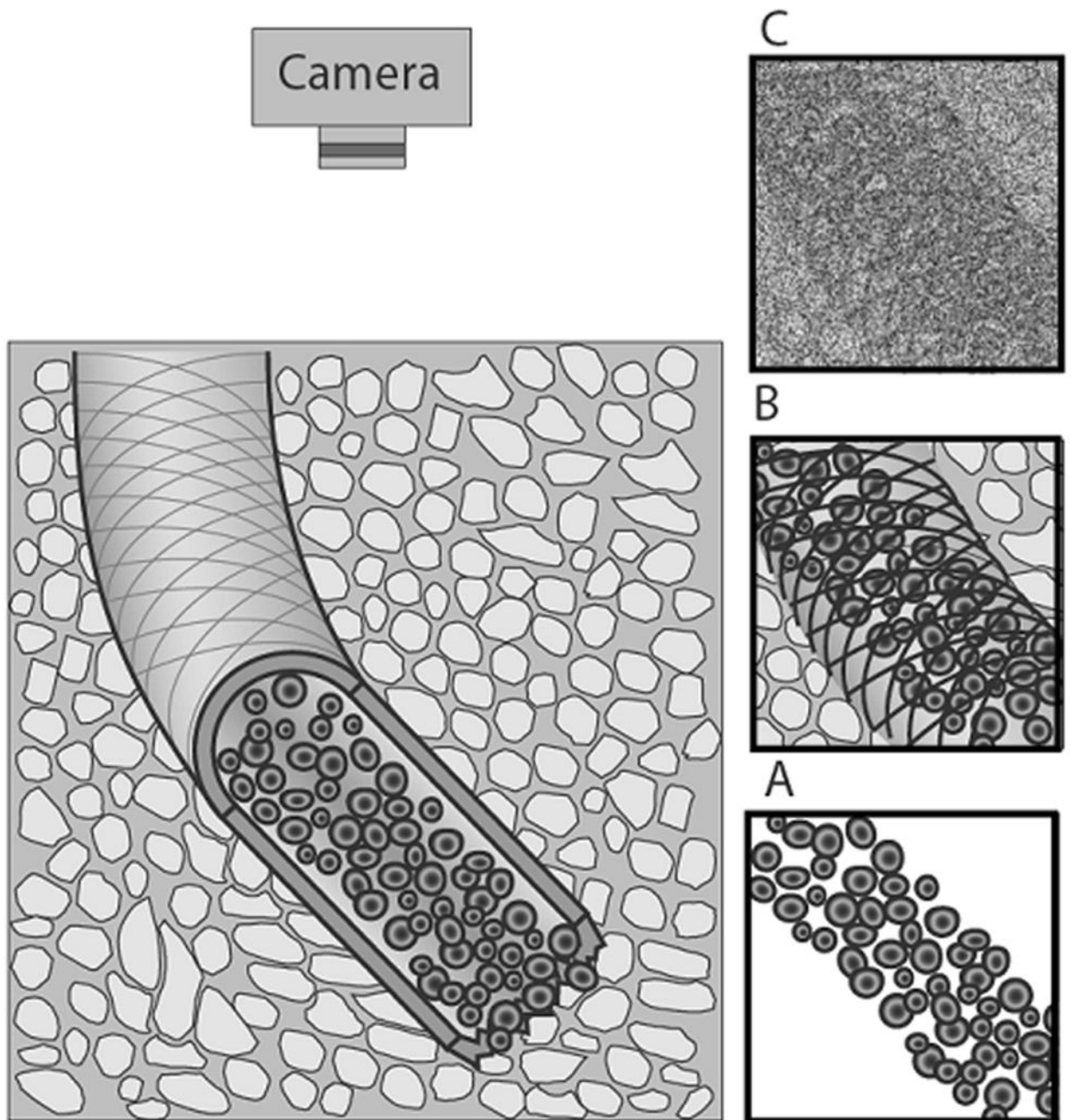
Figure 2.
Physical source of optical signals (left) and images containing those signals (right). The optical signal from moving blood cells (A) is obscured by the signal from stationary objects such as the blood vessel wall (B) and camera noise (C). Figure is not drawn to scale.
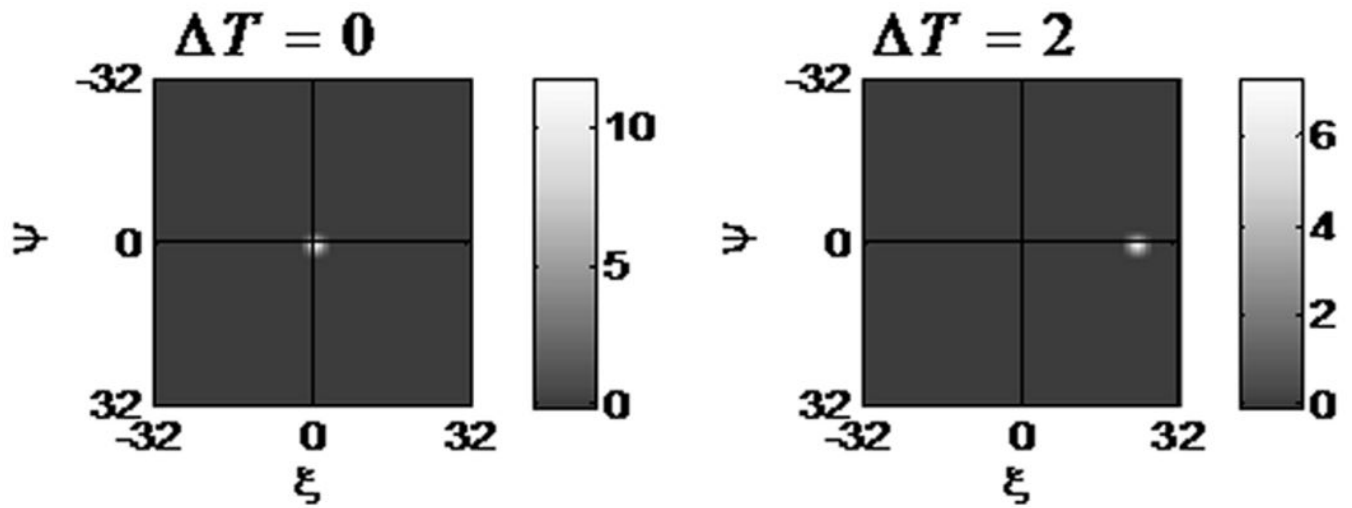
Figure 3.
STICS analysis of simulated data plotted at two STICS shifts (and frames). The simulated data has a velocity of 10pixels/frame and this is reflected in the STICS peak shift of 20 pixels.
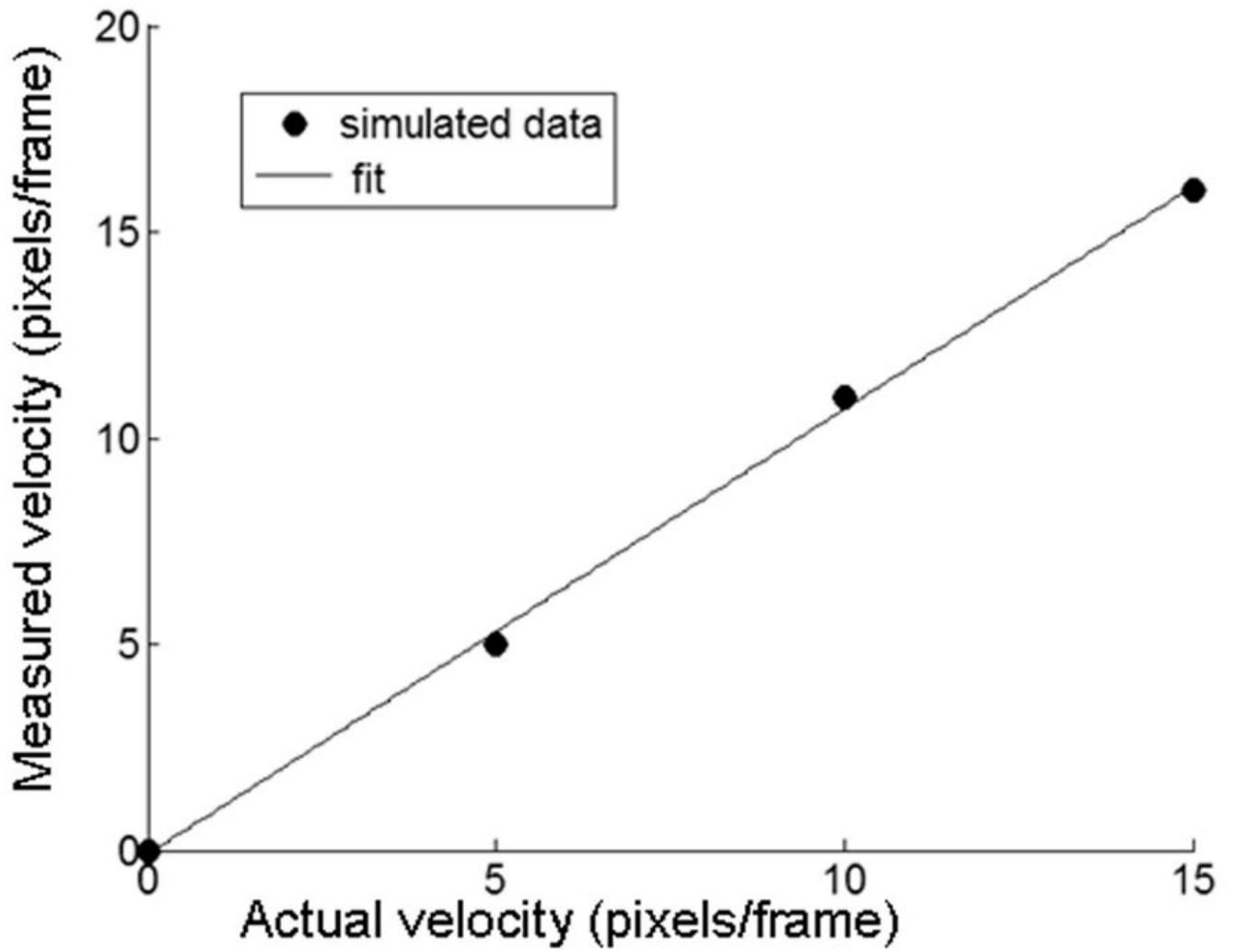
Figure 4.
Measured velocity versus simulated velocity. Velocity was calculated as described in equation 2.
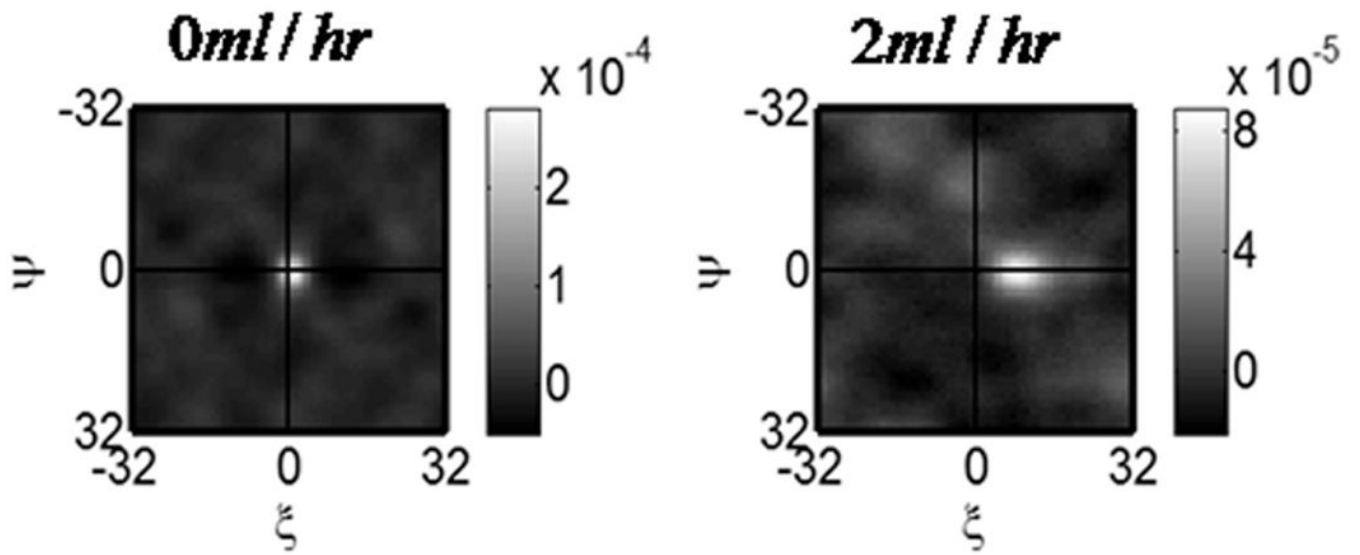
Figure 5.
STICS results for a shift of 5 frames and at two flow rates. As the flow rate increases the location of the STICS peak shifts in the direction of flow.
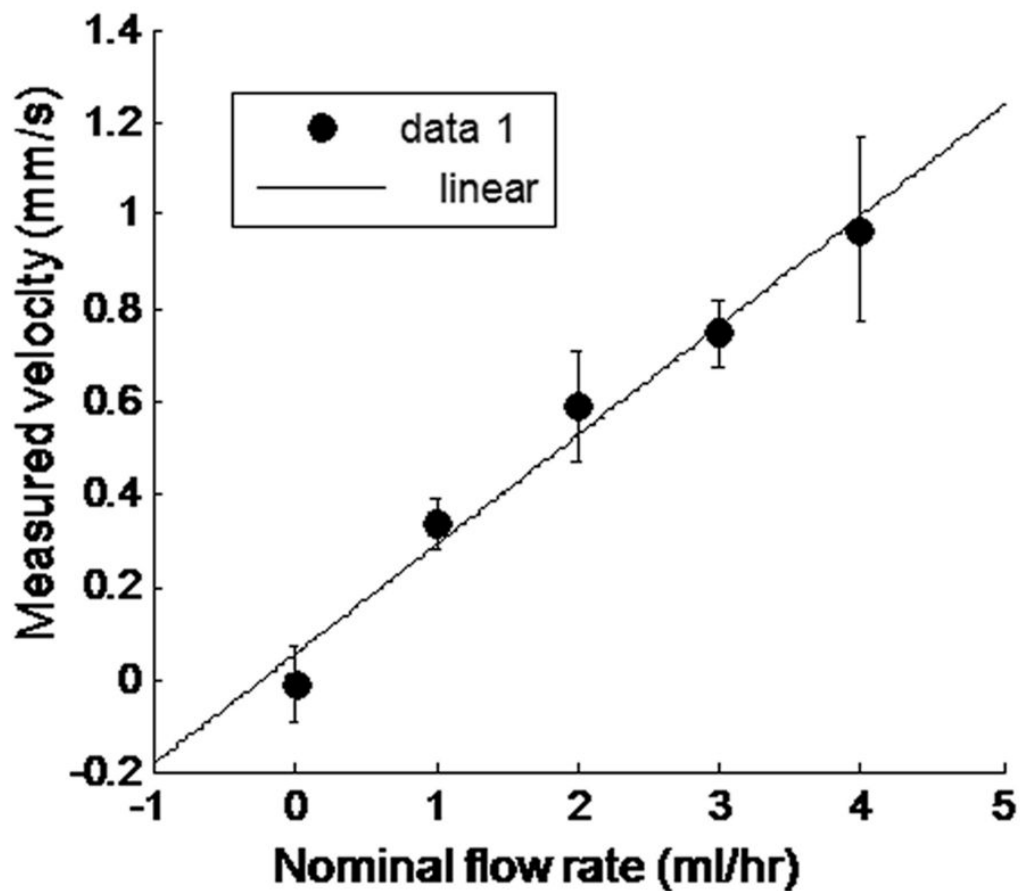
Figure 6.
Velocity measured using NIR-STICS versus the nominal flow rate. The flow rate reported by the syringe pump was faster than the actual flow rate by a factor of approximately 5 due to impedance in the microfluidic system. The results of 5 trials at each flow rate are plotted here.
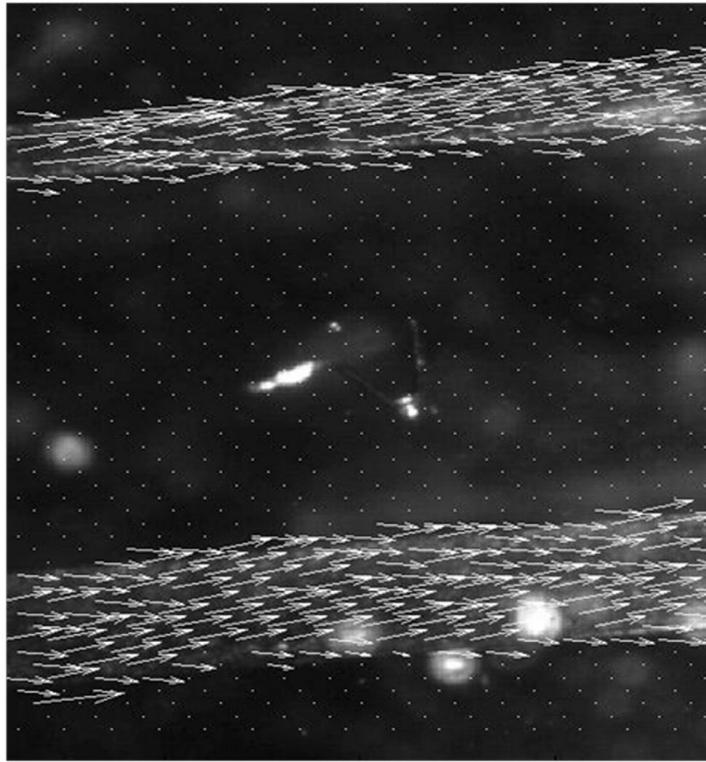
Figure 7.
STICS analysis for two different microchannels in the same image with the calculated flow rate represented as arrows. Analysis was performed in region 32 pixels by 32 pixels that overlapped by 16 pixels. Arrows represent the direction and magnitude of the velocity. The average velocity is 3.9mm/s in the top channel and 2.6mm/s second in the bottom channel.
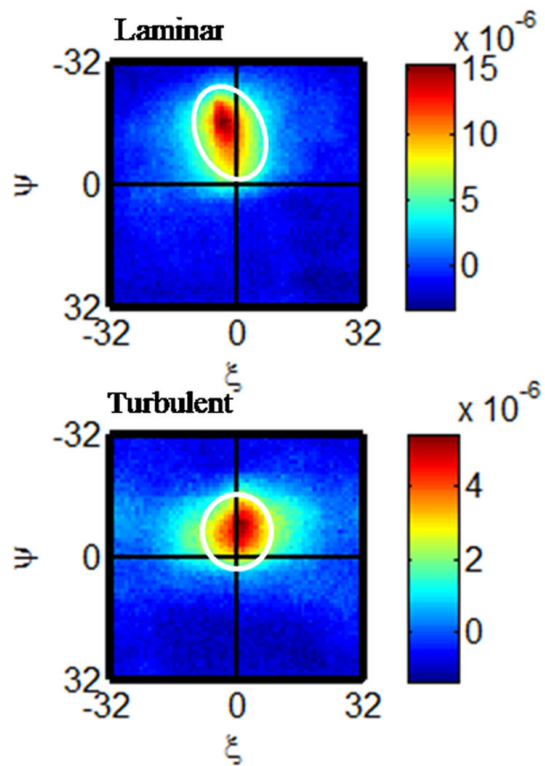
Figure 8.
STICS analysis of laminar and turbulent both at $\Delta T = 2$. Laminar flow is reflected in an elongated, asymmetrical STICS peak. The STICS peak for turbulent flow broadens in all directions. The white circles are included to identify the region of interest and are not computationally significant.